Parity nonconservation in ytterbium ion

B. K. Sahoo *
Theoretical Physics Division, Physical Research Laboratory, Ahmedabad-380009, India

B. P. Das
Theoretical Astrophysics Group, Indian Institute of Astrophysics, Bangalore-560034, India

(Dated: Received date; Accepted date)

We consider parity nonconservation (PNC) in singly ionized ytterbium (Yb^+) arising from the neutral current weak interaction. We calculate the PNC electric dipole transition amplitude ($E1_{PNC}$) and the properties associated with it using the relativistic coupled-cluster theory. $E1_{PNC}$ for the $[4f^{14}]\ ^26s \rightarrow [4f^{14}]\ ^25d_{3/2}$ transition in Yb^+ has been evaluated to within an accuracy of 5%. The improvement of this result is possible. It therefore appears that this ion is a promising candidate for testing the standard model of particle physics.

PACS numbers:

Parity nonconservation (PNC) has been observed in a number of neutral atoms; the latest being Yb [1, 2]. The combined experimental and theoretical results for Cs PNC is the most accurate to date [3]. It is in agreement with the standard model (SM) of particle physics. The experiment on Cs PNC also reports the observation of the nuclear anapole moment (NAM) [3, 4]. For more stringent tests of the SM, either the accuracy of the PNC data from Cs must be improved or very high precision measurements should be carried out on other candidates. Exploiting the remarkable advances in laser cooling and single ion trapping techniques, experiments have been proposed to measure PNC in these systems [5, 6]. Both Ba^+ [5, 6] and Ra^+ [7–9] are already under consideration for such experiments. Moreover, the PNC nucleon-nucleon coupling constant related to the NAM obtained from Cs PNC and nuclear data do not agree [4], and this clearly calls for further investigation of these results. In these circumstances, it would certainly be desirable to explore PNC in heavy atomic ions [9]. Apart from Ba^+ and Ra^+, we had also suggested Pb^+ as a possible candidate for PNC measurement [10]. The study of PNC in the $[4f^{14}]\ ^26s \rightarrow [4f^{14}]\ ^25d_{3/2}$ transition in Yb^+ was suggested by one of us over a decade ago [11] and it is currently being experimentally investigated at the Los Alamos National Laboratory [12].

Assuming that the PNC light-shift in the above transition in Yb^+ can be measured to sub one per cent accuracy, it would certainly be desirable to determine the accuracy to which $E1_{PNC}$ can be calculated for this transition. This knowledge is necessary for choosing a system for investigating atomic PNC. In alkali atoms and alkali earth-metal ions, the low-lying energy levels which are the singly excited states from the ground state usually make the dominant contributions to the $E1_{PNC}$ amplitude. Therefore, a typical sum-over-state approach considering only few important singly excited intermediate states can give a reasonably accurate result. However, Yb^+ has a number of doubly excited low-lying intermediate states, and therefore it would not be prudent to use a sum-over-states approach for this ion.

In this Rapid Communication, we employ the relativistic coupled-cluster (RCC) method to calculate $E1_{PNC}$ using an approach that circumvents summing over intermediate states [13]. We also present the results of our calculations of the excitation energies and the lifetimes for the $[4f^{14}]\ ^26p_{1/2,3/2}$ and the electric quadrupole moments of the $[4f^{14}]\ ^26s \rightarrow [4f^{14}]\ ^25d_{3/2}$ transition, which is necessary for evaluating the PNC light-shift associated with this transition in Yb^+. We analyze the role of the electron correlation effects in $E1_{PNC}$ and compare them with those in Ba^+ [13] and Ra^+ [7].

In Fig. 1, we present a diagram of the low-lying energy levels of Yb^+ mentioning lifetimes of the important states and transitions that can be induced by lasers for the measurement of PNC. As shown in the figure, the lifetimes of the $5d_{3/2,5/2}$ states are fairly large [14–16].

The largest contribution to $E1_{PNC}$ in the $[4f^{14}]\ ^26s \rightarrow [4f^{14}]\ ^25d_{3/2}$ transition comes from the nuclear spin independent (NSI) neutral weak current interaction between the electrons and the nucleus due to the exchange of Z_0 boson. The Hamiltonian for this interaction is given by

$$H_{PNC} = \frac{G_F}{2\sqrt{2}} Q_W \gamma_5 \rho_{nuc}(r), \tag{0.1}$$

where $G_F (= 2.219 \times 10^{-14}$ in au) is the Fermi constant that quantifies the strength of the weak interaction, ρ_{nuc} is the nuclear density which is evaluated using the Fermi

*bijaya@prl.res.in

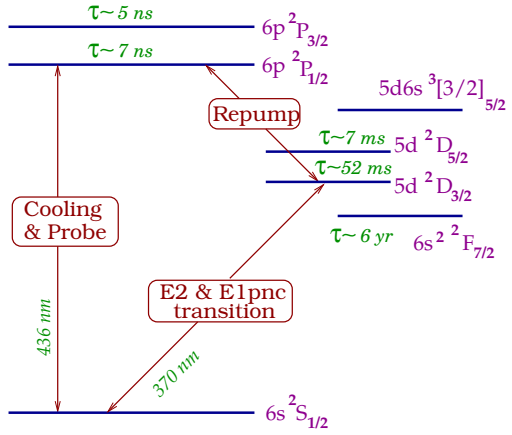

FIG. 1: (color online) A schematic diagram of energy levels in Yb^+ with transitions shown in red lines that can be induced by different lasers for the measurement of parity nonconservation effect. Lifetimes of different states are denoted by τ.

distribution, γ_5 is the Dirac matrix, N is the neutron number of the atomic system and Q_W is known as the weak nuclear charge. As the strength of the weak interaction is very small compared to the electromagnetic interactions in an atomic system, it can be treated as a first order perturbation. The wave function of an atomic state with a single valence electron v can be expressed as

$$|\Psi_v\rangle = |\Psi_v^{(0)}\rangle + G_F|\Psi_v^{(1)}\rangle, \tag{0.2}$$

with G_F representing the perturbed parameter, $|\Psi_v^{(0)}\rangle$ and $|\Psi_v^{(1)}\rangle$ are the wave functions corresponding to the the Dirac-Coulomb Hamiltonian (H_{DC}) and its first order correction due to the PNC weak interaction, respectively. In our RCC approach, we write

$$|\Psi_v\rangle = e^T[1+S_v]|\Phi_v\rangle, \tag{0.3}$$

where $|\Phi_v\rangle$ is the Dirac-Fock (DF) wave function obtained by appending the valence electron v to the closed-shell configuration reference state $|\Phi_0\rangle$ that is $[4f^{14}]$ in the present system and T and S_v are the core-virtual and valence-virtual excitation operators, respectively. In this work, we have considered all possible single and double excitations (CCSD method) by taking the operators

$$T = T_1 + T_2 \quad \text{and} \quad S_v = S_{1v} + S_{2v}, \tag{0.4}$$

where subscripts 1 and 2 stand for the single and double excitations, respectively. We also consider contributions from triple excitations involving the valence electron by defining the following operator

$$S_{3v} = \frac{H_{DC}T_2 + H_{DC}S_{2v}}{\varepsilon_p + \varepsilon_q + \varepsilon_r - \varepsilon_v - \varepsilon_a - \varepsilon_b}, \tag{0.5}$$

where ε represents the orbital energy and p, q, r and a, b represent the virtual and occupied orbitals, respectively. When S_{3v} is used only to improve the CCSD wave functions, it is referred to as the CCSD(T) method and when its contributions are also estimated then it is known as lo-CCSDvT method [17]. Further, we separate the T and S_v operators to represent the unperturbed and perturbed wave functions as

$$T = T^{(0)} + G_F T^{(1)} \quad \text{and} \quad S_v = S_v^{(0)} + G_F S_v^{(1)}, \tag{0.6}$$

where the superscripts 0 and 1 denote unperturbed and perturbed operators, respectively. In an explicit form, we can write

$$|\Psi_v^{(0)}\rangle = e^{T^{(0)}}[1+S_v^{(0)}]|\Phi_v\rangle \tag{0.7}$$

$$\text{and} \quad |\Psi_v^{(1)}\rangle = e^{T^{(0)}}[T^{(1)}(1+S_v^{(0)}) + S_v^{(1)}]|\Phi_v\rangle. \tag{0.8}$$

The RCC equations for the correlation energy and the cluster amplitudes equations for both the unperturbed and perturbed wave functions have been given in some of our earlier papers (for example see [13, 17]).

An atomic property can be determined in the RCC framework by evaluating the matrix element of an operator O corresponding to that property

$$\langle O\rangle_{fi} = \frac{\langle\Phi_f|[1+S_f^{(0)^\dagger}]\mathcal{O}_0[1+S_i^{(0)}]|\Phi_i\rangle}{\sqrt{\mathcal{N}_f\mathcal{N}_i}}, \tag{0.9}$$

where $\mathcal{O}_0 = e^{T^{(0)^\dagger}}Oe^{T^{(0)}}$ and $\mathcal{N}_v = \langle\Phi_v|[1+S_v^{(0)^\dagger}]\mathcal{N}_0[1+S_v^{(0)}]|\Phi_v\rangle$ with $\mathcal{N}_0 = e^{T^{(0)^\dagger}}e^{T^{(0)}}$. Expectation values are determined by taking $f = i$.

The expression for $E1_{PNC}$ between $|\Psi_f\rangle$ and $|\Psi_i\rangle$ after keeping terms up to linear in G_F is given by

$$E1_{PNC} = G_F\frac{\langle\Psi_f^{(0)}|D|\Psi_i^{(1)}\rangle + \langle\Psi_f^{(1)}|D|\Psi_i^{(0)}\rangle}{\sqrt{\langle\Psi_f^{(0)}|\Psi_f^{(0)}\rangle\langle\Psi_i^{(0)}|\Psi_i^{(0)}\rangle}}, \tag{0.10}$$

for the electric dipole (E1) operator D, which in the RCC approach leads to

$$\frac{E1_{PNC}}{G_F} = \frac{\langle\Phi_f|[1+S_f^{(0)^\dagger}]\mathcal{D}_0[T^{(1)}(1+S_i^{(0)}) + S_i^{(1)}]|\Phi_i\rangle}{\sqrt{\mathcal{N}_f\mathcal{N}_i}} + \frac{\langle\Phi_f|[S_f^{(1)^\dagger} + (1+S_f^{(0)^\dagger})T^{(1)^\dagger}]\mathcal{D}_0[1+S_i^{(0)}]|\Phi_i\rangle}{\sqrt{\mathcal{N}_f\mathcal{N}_i}}.$$

In Table I, we present results for different properties using our CCSD(T) method. The results for the appropriate properties can be used for estimating the uncertainty of our $E1_{PNC}$ result. We also compare our results with previous calculations and experimental results wherever possible. We analyze the results briefly below.

Basis functions: We have considered up to 17 s, p, d and f and 14 g orbitals using Gaussian type orbital basis functions. A Fermi-nuclear charge distribution is used to determine the nuclear potential and density.

Excitation energies: We have given excitation energies (EEs) in Table I corresponding to the transitions that are important in obtaining an accurate value for $E1_{PNC}$ result and the lifetimes of excited states. Among them EE

TABLE I: Comparison of different properties in $^{171}Yb^{+}$ from the present and other works (given up to second decimal place). Uncertainties are given inside the parentheses.

Properties	This work	Others	Experiment
Transitions	Excitation energies (in cm^{-1})		
$6s_{1/2} \rightarrow 6p_{1/2}$	28109(1000)	28048[a]	27061.82[b]
$6s_{1/2} \rightarrow 6p_{3/2}$	31604(800)	31411[a]	30392.23[b]
$6s_{1/2} \rightarrow 7p_{1/2}$	63518(200)	63227[a]	63706.25[b]
$6p_{1/2} \rightarrow 5d_{3/2}$	4879(800)	6810[a]	4101.02[b]
$6p_{3/2} \rightarrow 5d_{3/2}$	8375(950)	10173[a]	7431.43[b]
$6p_{3/2} \rightarrow 5d_{5/2}$	7015(1000)	8962[a]	6059.54[b]
$7p_{3/2} \rightarrow 5d_{3/2}$	41502(1500)	43175[a]	42633.30[b]
	E1 matrix elements (in au)		
$6s_{1/2} \rightarrow 6p_{1/2}$	2.72(1)	2.68/2.73[a], 2.76[c]	
$6s_{1/2} \rightarrow 6p_{3/2}$	3.83(1)	3.77/3.84[a], 3.87[c]	
$6s_{1/2} \rightarrow 7p_{3/2}$	0.18(2)	0.15/0.04[a]	
$6p_{1/2} \rightarrow 5d_{3/2}$	3.06(2)	2.97/3.78[a], 3.19[c]	
$6p_{3/2} \rightarrow 5d_{3/2}$	1.35(2)	1.31/1.55[a], 1.40[c]	
$6p_{3/2} \rightarrow 5d_{5/2}$	4.23(3)	4.12/4.77[a], 4.39[c]	
$7p_{1/2} \rightarrow 5d_{3/2}$	0.17(2)	0.08/0.12[a]	
	E2 matrix elements (in au)		
$6s_{1/2} \rightarrow 5d_{3/2}$	10.2(5)		
$6s_{1/2} \rightarrow 5d_{5/2}$	12.9(7)		12(1)
States	A_{hyf} constants (in MHz)		
$6s_{1/2}$	13332(1000)	13172[a], 12730[d]	12645(2)[d]
$6p_{1/2}$	2516(400)	2350[a], 2317[d]	2104.9(1.3)[d]
$6p_{3/2}$	322(20)	311.5[a], 391[d]	877(20)[e]
$7p_{1/2}$	861(50)	807.4[a]	
$7p_{3/2}$	123(15)	110.8[a]	
$5d_{3/2}$	447(20)	400.48[f]	430(43)[g]
$5d_{5/2}$	−48(15)	−12.58[f]	−63.6(7)[h]

References: [a][18]; [b][19]; [c][21]; [d][23]; [e][24]; [f][25]; [g][26]; [h][27].

of the $6s_{1/2} \rightarrow 6p_{1/2}$ transition contribute significantly to the $E1_{PNC}$ result which is obtained to an accuracy of around 4% in this work. All our results are compared with MBPT(3) results of Safronova and Safronova [18] and also with experimental values [19].

E1 matrix elements: It is important to find the accuracy of the E1 matrix elements that contribute to $E1_{PNC}$. We have presented the important E1 matrix elements in the above table. Our results compare reasonably well with previous calculations [18, 20]. In [18], two different approaches were considered to obtain these results which differ from each other substantially. We have compared our results with Mani and Angom (their published results [20] have been corrected [21]). We combine our E1 matrix elements with the experimental wavelengths to determine the lifetimes of the important intermediate states; $6p\ ^2P_{1/2}$ and $6p\ ^2P_{3/2}$ states and compare them with the measured values in order to test their accuracies. Using our calculated E2 and M1 amplitudes; i.e.

TABLE II: $E1_{PNC}$ results in Yb^{+} in $10^{-11} iea_0(-Q_W/N)$ using different approximations.

Result \ Method	DF	CCSD	CCSD(T)	lo-CCSDvT
$E1_{PNC}$	6.5311	8.5126	8.4702	8.4704

20.70 au and 1.15 au, respectively for the $6p_{3/2} \rightarrow 6p_{1/2}$ transition, we find lifetimes of the $6p\ ^2P_{1/2}$ and $6p\ ^2P_{3/2}$ states as 6.70 ns and 4.75 ns, which agree reasonably with the experimental results 7.1(4) ns and 5.5(3) ns of Blagoev et al [22], respectively. Also, the branching ratio of the decay rate of the $6p\ ^2P_{1/2}$ state to the $5d\ ^2D_{3/2}$ state has been reported as 0.0483 with 9% uncertainty [15] and it agrees well with our result 0.0439.

E2 matrix elements: We have also determined the E2 matrix elements of the $6s_{1/2} \rightarrow 5d_{3/2}$ and $6s_{1/2} \rightarrow 5d_{5/2}$ transitions which are needed in evaluating the PNC light shift. No other results are available for comparison. Taylor et al have measured the lifetimes of the $5d\ ^2D_{5/2}$ state as 7.2(3) ms with a branching ratio to the $^2F_{7/2}$ state of 0.83(3) [16]. From their measurements, we estimate the E2 matrix element of the $6s_{1/2} \rightarrow 5d_{5/2}$ transition as 12(1) au and our result is in agreement with that. Therefore, we expect that our E2 transition amplitude for the $6s_{1/2} \rightarrow 5d_{3/2}$ transition will also be of similar accuracy.

Hyperfine structure constants: We have presented the magnetic dipole hyperfine structure constants (A_{hyf}) of the low-lying singly excited states of $^{171}Yb^{+}$. They are also compared with other calculations and experimental results. Our results are comparatively larger than the experimental values, but all the measurements are relatively old. A large disagreement between experimental and all theoretical results of the $6p\ ^2P_{3/2}$ state calls for verification of these results using new experimental techniques. However, the accuracies of our results for obtaining a reasonable estimate of $E1_{PNC}$ are currently acceptable. For high precision results, it would be necessary to improve the accuracies of the calculations.

$E1_{PNC}$ result: We turn here to our $E1_{PNC}$ calculation of the $6s_{1/2} \rightarrow 5d_{3/2}$ transition where the correlation effects seem to be significant. It can be seen from Table II that the $E1_{PNC}$ result increases by 30% and 29% at the CCSD and CCSD(T) levels, respectively. So there are some cancellations between the correlation contributions coming via the CCSD and CCSD(T) methods.

We now proceed to discuss the trends of the correlation effects by considering the contributions from different RCC terms. In Table III, we give contributions from the DF and individual CCSD(T) terms. By relating the important CCSD(T) terms to their corresponding lower order MBPT counterparts, we can identify the correlations effects that are significant. As seen in Table III, three different classes of RCC terms are of crucial importance in arriving at the final result. The $\mathcal{D}_0 T_1^{(1)}$ term

TABLE III: Contributions (Contr.) to $E1_{PNC}$ result (in $\times 10^{-11} ie a_0(-Q_W/N)$) in Yb^+ at the DF and CCSD(T) methods as initial ($i = 6s\ ^2S_{1/2}$) and final ($f = 5d\ ^2D_{3/2}$) perturbed states. Results given as $Norm$ and $Others$ refer to contributions from normalization of the wave functions and RCC terms those are not mentioned explicitly, respectively. Subscripts c and vir represent contributions from core and virtual orbitals, respectively.

Method	Initial state	Contr.	Final state	Contr.
DF	$(H_{PNC}D)_c$	0.6441	$(DH_{PNC})_c$	-3.3×10^{-7}
	$(DH_{PNC})_{vir}$	5.8870	$(H_{PNC}D)_{vir}$	-4.3×10^{-5}
RCC	$T_1^{(1)\dagger}\mathcal{D}_0$	0.6745	$\mathcal{D}_0T_1^{(1)}$	0.0070
	$\mathcal{D}_0S_{1i}^{(1)}$	7.1973	$S_{1f}^{(1)\dagger}\mathcal{D}_0$	1.3424
	$\mathcal{D}_0S_{2i}^{(1)}$	−0.2929	$S_{2f}^{(1)\dagger}\mathcal{D}_0$	−0.2022
	$S_{1f}^{(0)\dagger}\mathcal{D}_0S_{1i}^{(1)}$	0.5115	$S_{1f}^{(1)\dagger}\mathcal{D}_0S_{1i}^{(0)}$	−0.0788
	$S_{2f}^{(0)\dagger}\mathcal{D}_0S_{1i}^{(1)}$	−0.3682	$S_{1f}^{(1)\dagger}\mathcal{D}_0S_{2i}^{(0)}$	−0.0617
	$S_{1f}^{(0)\dagger}\mathcal{D}_0S_{2i}^{(1)}$	0.0004	$S_{2f}^{(1)\dagger}\mathcal{D}_0S_{1i}^{(0)}$	−0.0165
	$S_{2f}^{(0)\dagger}\mathcal{D}_0S_{2i}^{(1)}$	0.0271	$S_{2f}^{(1)\dagger}\mathcal{D}_0S_{2i}^{(0)}$	0.0096
	$Others$	−0.6261		0.7078
	$Norm$	-0.2911		−0.0670

represents a sub class of core-valence correlations, whose contribution in the present case is slightly larger than DF result that is denoted as $(DH_{PNC})_c$. As we have previously discussed [13, 17], $\mathcal{D}_0S_{1v}^{(1)}$ effectively considers contributions from singly excited states with $(DH_{PNC})_{vir}$ as its leading term and involves contributions from important pair-correlation and a class of core-polarization effects. Clearly this contribution through the perturbed $5d\ ^2D_{3/2}$ state at the DF level is negligible, but after including electron correlation effects, its contribution becomes large. The other important contributions coming via $\mathcal{D}_0S_{2v}^{(1)}$ are from the core polarization effects involving doubly excited states such as $4f^{13}\ (^2F_{5/2})\ 6s^2$ and $4f^{13}\ (^2F_{7/2})\ 5d6s$. A sizable amount of contribution comes collectively from certain higher order RCC terms given as $Others$. Contributions from the normalization of the wave functions (given as $Norm$) are also not small.

A detailed comparative study of the trends of the correlation effects in $E1_{PNC}$ amplitudes of the $s_{1/2} \rightarrow 5d_{3/2}$ transitions in Yb^+ and similar transitions in Ba^+ and Ra^+ will be reported elsewhere. However, there is an important point that we would like to highlight here. There is a cancellation between $\mathcal{D}_0S_{1v}^{(1)}$ and its complex conjugate (cc) term in Ba^+ and Ra^+, but in contrast in the present case it adds up. Therefore, the net correlation contribution is larger in Yb^+ than other two ions.

Analysing results from Table III, we find that the leading contributions from $\mathcal{D}_0T^{(1)} + cc$ through the core electrons, $[\mathcal{D}_0S_{1i}^{(1)} + S_{1f}^{(0)\dagger}\mathcal{D}_0S_{1i}^{(1)}] + cc$ as in the form of the single excitations of the valence electrons and the double excitation terms $[\mathcal{D}_0S_{2i}^{(1)} + S_{1f}^{(0)\dagger}\mathcal{D}_0S_{2i}^{(1)} + S_{2f}^{(0)\dagger}\mathcal{D}_0S_{2i}^{(1)}] + cc$ are around 8%, 101% and 9% (with opposite sign), respectively. The uncertainties in the contributions from the core and doubly excited states are taken as the differences of the CCSD and lo-CCSD(T) results. Uncertainties from the singly excited states are estimated from the errors of various physical quantities which are given in Table I and taking into account their contributions with appropriate weights. With those uncertainties, we estimate the $E1_{PNC}$ amplitude for the $6s\ ^2S_{1/2} \rightarrow 5d\ ^2D_{3/2}$ transition in Yb^+ to be $8.5(5)\times10^{-11}\ iG_F e a_0(-Q_W/N)$. The results can be improved by including the triple and quadruple hole-particle excitations in the framework of general-order RCC theory [28].

In conclusion,Yb^+ appears to be a promising candidate for the study of atomic PNC. By employing the RCC method in the singles, doubles and partial triples approximation, we have estimated various atomic properties including the $E1_{PNC}$ amplitude. Our preliminary investigation suggests that it is feasible to obtain theoretical results in this system with high accuracy after suitable modifications to our present method which has yielded a result that is about 5% accurate. A different trend for correlation effects is found in the present case than Ba^+ and Ra^+; the two ions that were previously studied using the same method.

We thank J. R. Torgerson for communicating with us. The computation of the results presented in this work were obtained using PRL HPC 3TFLOP cluster.

[1] J. S. M. Ginges and V. V. Flambaum, Phys. Rep. **637**, 63 (2004).
[2] K. Tsigutkin *et al*, Phys. Rev. Lett. **103**, 071601 (2009).
[3] C. S. Wood *et al*, Science **275**, 1759 (1997).
[4] W. C. Haxton and C. E. Wieman, Ann. Rev. Nucl. Part. Sci. **51**, 261 (2001).
[5] N. Fortson, Phys. Rev. Lett. **70**, 2383 (1993).
[6] P. Mandal and M. Mukherjee, Phys. Rev. A **82**, 050101(R) (2010).
[7] L. W. Wansbeek *et al*, Phys. Rev. A **78**, 050501(R) (2008).
[8] O. O. Versolato *et al* , Phys. Rev. A **82**, 010501(R) (2010).
[9] B. K. Sahoo *et al*, Phys. Rev. A **83**, 030502(R) (2011).
[10] B. K. Sahoo *et al*, Phys. Rev. A **72**, 032507 (2005).
[11] B. P. Das, *Proceedings of the Workshop on Violations of Fundamental Symmetries in Atoms and Nuclei*, INT, Seattle, 1999 (unpublished).
[12] J. R. Torgerson, *Private communication*.
[13] B. K. Sahoo *et al*, Phys. Rev. Lett. **96**, 163003 (2006).
[14] Ch. Gerz *et al*, Z. Phys. D **8**, 235 (1988).
[15] N. Yu and L. Laleki, Phys. Rev. A **61**, 022507 (2000).
[16] P. Taylor *et al*, Phys. Rev. A **56**, 2699 (1997).
[17] B. K. Sahoo, J. Phys. B **43**, 085005 (2010).

[18] U. I. Safronova and M. S. Safronova, Phys. Rev. A **79**, 022512 (2009).
[19] http://physics.nist.gov/cgi-bin/ASD/energy1.pl
[20] B. K. Mani and D. Angom, Phys. Rev. A **83**, 012501 (2011).
[21] B. K. Mani and D. Angom, *Private communication*.
[22] K. B. Blagoev *et a*/, Opt. Spectrosc. **45**, 832 (1978).
[23] A.-M. Mårtensson-Pendrill *et al*, Phys. Rev. A **49**, 3351 (1994).
[24] R. W. Berends and L. Maleki, J. Opt. Soc. Am. B **9**, 332 (1992).
[25] W. M. Itano, Phys. Rev. A **73**, 022510 (2006).
[26] D. Engelke and C. Tamm, Europhys. Lett. **33**, 347 (1996).
[27] W. Roberts *et al*, Phys. Rev. A **60**, 2867 (1999).
[28] M. Kállay *et al*, Phys. Rev. A **83**, 030503(R) (2011).